Comparison of DAFH and FALDI-like approaches

David L. Cooper[1] • Jurgens de Lange[2] • Robert Ponec[3]

✉ David L. Cooper

dlc@liverpool.ac.uk

✉ Jurgens de Lange

jurgens.delange@up.ac.za

✉ Robert Ponec

ponec@icpf.cas.cz

1   Department of Chemistry, University of Liverpool, Liverpool L69 7ZD, UK

2   Theoretical Chemistry, Department of Chemistry, Faculty of Natural and Agricultural Sciences, University of Pretoria, Gauteng, South Africa

3   Institute of Chemical Process Fundamentals, Czech Academy of Sciences Prague 6, Suchdol 2, 165 02 Czech Republic

Abstract

Two complementary methodologies for extracting useful insights into electronic structure and bonding from contemporary wavefunctions are compared. The first of these, known as the analysis of domain-averaged Fermi holes (DAFH) mostly provides visually appealing descriptions of the role and the extent of electron sharing in chemical bonding. The second one, known as the fragment, atom, localized, delocalized and interatomic (FALDI) charge density decomposition scheme, uses the partitioning of certain localization and delocalization indices to focus on highly visual contributions associated with individual domains and with pairs of domains, respectively. Four variants of a FALDI-like approach are investigated here in some detail, mostly to establish which of them are the most reliable and the most informative. In addition to 'full' calculations that use the correlated pair density, the consequences for the DAFH and FALDI-like procedures of using instead a popular one-electron approximation are explored. Additionally, the geometry dependence of the degree of acceptability of the errors that this introduces for delocalization indices is assessed for different formal bond multiplicities. The familiar molecular test systems employed for these various linked investigations are the breaking of the bonds in H_2 and in N_2, as well as the nature of the bonding in B_2H_6, as a simple example of multicenter bonding. One of the key outcomes of this study is a clear understanding of how DAFH analysis and a particular variant of FALDI-like analysis could be most profitably deployed to extract complementary insights into more complex and/or controversial bonding situations.

---

1 Introduction

Advances in understanding electronic structure and bonding continue to rely not only upon the development and application of computational strategies for carrying out accurate calculations, but also upon the development and application of reliable techniques for extracting useful insights from contemporary calculations. Some six decades ago, Charles Coulson suggested that a key role of quantum chemistry is to understand concepts and to show what are the essential features of chemical behavior [1] and the motto of Richard Hamming's textbook on numerical methods is that the purpose of computing is insight, not numbers [2]. Eugene Wigner has often been quoted as saying: "It is nice to know that the computer understands the problem. But I would like to understand it too." Somewhat more recently, Frank Neese and co-workers have reminded all of us that nowadays we need both the insights *and* the numbers [3].

Unsurprisingly an impressive array of techniques has been developed for extracting useful chemical insights from contemporary calculations, even though some of the most useful concepts in electronic structure and bonding do tend to be difficult to pin down with unambiguous precise definitions. Examples of such broad families of approaches include various energy partitioning schemes, those which rely on partitioning densities and/or density matrices, conceptual density functional theory, and procedures for extracting descriptions of the valence bond type, just to mention but a few. Often it turns out that combinations of techniques give the most useful and reliable insights, with one such example being EDA-NOCV [4,5] which combines a particular form of energy decomposition analysis with highly visual natural orbitals for chemical valence. In the present work we focus on two methodologies that are linked to the partitioning of density matrices, with one of the aims being to find a combination in which they provide complementary useful information.

The two methodologies considered here have both proved to be particularly useful for visualizing the actual bonding situation in molecular systems. One of them is domain-averaged Fermi hole (DAFH) analysis [6-14] which is especially useful for the manner in which it depicts the role and the extent of electron sharing in bonding situations. The other is linked to the original fragment, atom, localized, delocalized and interatomic (FALDI) charge density decomposition scheme [15-19]. The FALDI scheme provides, amongst other things, information about the partitioning of shared electrons into the contributions of individual bonded atoms.

In essence DAFH analysis involves integration over a chosen domain of one of the electron coordinates in the exchange–correlation density, $\rho_{xc}(\mathbf{r}_1, \mathbf{r}_2)$, so as to generate a one-electron quantity that can loosely be labelled a 'hole'. Although the eigenvectors and associated eigenvalues of a matrix

representation of that 'hole' could in principle be interpreted directly as domain natural orbitals, they are more usually transformed using an isopycnic (meaning 'same density') localization procedure [20]. Examination of the forms of the resulting (nonorthogonal) one-electron DAFH functions and their corresponding occupation numbers then provides highly visual interpretations of chemical bonding. In general it proves to be particularly useful to perform DAFH analysis for 'holes' that are averaged over (combinations of) individual quantum theory of atoms in molecules (QTAIM) [21] domains.

Except for the special case of closed-shell restricted Hartree-Fock wavefunctions, the actual construction of $\rho_{xc}(\mathbf{r}_1, \mathbf{r}_2)$ does of course require use of the pair density, which is not always readily available. Fortunately it has been shown that the significant simplifications that arise from the use instead of a convenient one-electron approximation do not lead to significant changes in the forms of the dominant DAFH functions [22], but there are modest changes to the associated occupation numbers.

Integration of the 'hole' over the same or a different domain generates quantities known as localization and delocalization indices [23], respectively. Bader argued that the information provided by these delocalization indices is independent of any association with chemical bonding between the atoms involved and, as such, the delocalization index should not be identified as a bond order [23]. Furthermore, it was argued that the delocalization index does not determine the number of Lewis-bonded pairs [23], except in the special case of equally-shared electron pairs. Nonetheless such delocalization indices have been widely used as bond orders or as surrogates for bond orders in a wide variety of applications. In particular, it has been strongly suggested relatively recently in a study of nearly 200 inorganic and organic molecules that such delocalization measures in real space could be used to revitalize the whole concept of bond order [24].

Whether or not it should actually be considered a bond order, the delocalization index is clearly an example of an electron sharing index [25], quantifying the extent of the sharing of the electron distribution between two QTAIM domains. Accordingly we have chosen to use instead the term shared-electron distribution index (SEDI) [26], thereby also avoiding any possible confusion with alternative delocalization measures or electron sharing indices. Indeed, purely for convenience, we will refer to the corresponding localization indices as diagonal SEDI values, whereas the off-diagonal ones are of course delocalization indices. It proves straightforward to resolve such values of SEDI into contributions that involve individual DAFH functions [27] (see also [12,13]).

The original FALDI scheme [15-19] quantifies pseudo-second-order contributions arising from electrons within QTAIM domains. One of its outcomes is in essence a means of visualizing SEDI values (albeit calculated within the usual one-electron approximation) in terms of sets of one-electron functions and their associated eigenvalues. We note that it has been found that whereas the significant

simplifications provided by the one-electron approximation introduce errors in off-diagonal SEDI values that are less than 5% for many bonds, the corresponding errors for high bond multiplicities, such as the formal triple bonds in N_2 and HCN, can exceed 10% [24]. Provided that it is readily available, it would of course be straightforward to avoid the one-electron approximation that is implicit in the original formulations of FALDI [15-19] by using instead the actual pair density; we could also choose to localize the resulting one-electron functions by means of an isopycnic transformation [20], exactly as in DAFH analysis. The variants of FALDI considered here have been labelled FALDI-like, to distinguish them from the original, but it is our expectation that any lessons learnt here can be carried back to the original formulation.

The main purpose of the present work is to try to provide answers to a series of interrelated questions associated with DAFH analysis, the FALDI-like approach and SEDI values:

- For the different variants of the FALDI-like approach, as explained later, which are the most useful?
- How similar/different are the functions generated by the DAFH and FALDI-like approaches for a particular molecule at a given level of theory and how similar/different are the corresponding eigenvalues?
- Is there a combination of the DAFH and FALDI-like approaches in which they provide complementary useful information?
- Can the FALDI-like approach give a more compact (or more 'efficient') expansion of SEDI values than does DAFH analysis?
- Given the extent to which use of the usual one-electron approximation has been shown to affect SEDI values [24], would its use in the DAFH and FALDI-like approaches affect also the *relative* importance of the different functions in the expansions of SEDI values?
- Do the answers to any of the above questions depend on the formal bond multiplicity and do any of the answers change for a given system when nuclear separations are increased/decreased?

Along the way we also examine for representative systems the extent to which the accuracy of the one-electron approximation for calculating SEDI values varies with nuclear separation.

2 Theoretical and computational details

A convenient starting point for introducing DAFH analysis is to define the 'hole' g_Ω for a particular domain Ω as follows:

$$
\begin{aligned}
g_\Omega(\pmb{r}_1, \pmb{r}_1') \;=&\; \underset{\substack{r_2=r_2' \\ \Omega}}{\int} \rho_{\mathrm{xc}}(\pmb{r}_1, \pmb{r}_1'; \pmb{r}_2, \pmb{r}_2') d\pmb{r}_2 \\[2mm]
=&\; \rho^{(1)}(\pmb{r}_1, \pmb{r}_1') \underset{\substack{r_2=r_2' \\ \Omega}}{\int} \rho^{(1)}(\pmb{r}_2, \pmb{r}_2') d\pmb{r}_2 - 2 \times \underset{\substack{r_2=r_2' \\ \Omega}}{\int} \rho^{(2)}(\pmb{r}_1, \pmb{r}_1'; \pmb{r}_2, \pmb{r}_2') d\pmb{r}_2 \\[2mm]
\equiv&\; \sum_I \sum_J \phi_I(\pmb{r}_1) G_\Omega(I,J) \phi_J(\pmb{r}_1')
\end{aligned}
$$

$$(1)$$

in which $\rho^{(1)}$ and $\rho^{(2)}$ are spinless one- and two-electron densities and the ϕ_I are (real) orthonormal natural orbitals with occupation numbers ω_I. It is straightforward to construct this matrix representation $\mathbf{G}_\Omega$ of the 'hole' g_Ω by combining elements of the (spinless) one- and two-electron density matrices, expressed in this natural orbital basis, with so-called domain-condensed overlap integrals:

$$
S_\Omega(I,J) = \int_\Omega \phi_I(\pmb{r}_1) \phi_J(\pmb{r}_1) d\pmb{r}_1
$$

$$(2)$$

A convenient one-electron approximation that can be traced back to work by Müller [28], as well as to certain bond orders introduced by Fulton [29], has been rediscovered many times and continues to be used for various purposes, especially when the two-electron density is not readily available. This one-electron approximation, which is exact in the special case of closed-shell restricted Hartree-Fock wavefunctions, effectively reduces the expression for $G_\Omega(I,J)$ to $\sqrt{\omega_I \omega_J} S_\Omega(I,J)$.

Whether we do the full calculation using the pair density or we use instead the much simpler form based on the one-electron approximation mentioned above, the eigenvectors and eigenvalues of $\mathbf{G}_\Omega$ are transformed using an implementation of Cioslowski's isopycnic localization procedure [20], resulting for the chosen domain Ω in a set of (real) DAFH functions $\varphi_{i\Omega}$ with occupation numbers $n_{i\Omega}$. In effect, the so-called 'hole' g_Ω for domain Ω has been re-expressed in the following simple form

$$
g_\Omega(\pmb{r}_1, \pmb{r}_1') = \sum_i n_{i\Omega} \varphi_{i\Omega}(\pmb{r}_1) \varphi_{i\Omega}(\pmb{r}_1') = \sum_i \left(n_{i\Omega} \sum_{I,J} d_{i\Omega J} d_{i\Omega I} \phi_I(\pmb{r}) \phi_J(\pmb{r}_1') \right)
$$

$$(3)$$

in which the $d_{i\Omega I}$ are the expansion coefficient of the DAFH functions $\varphi_{i\Omega}$ in the basis of the natural orbitals ϕ_I:

$$\varphi_{i\Omega}(\boldsymbol{r}) = \sum_I d_{i\Omega I}\,\phi_I(\boldsymbol{r})$$

(4)

It is the inspection of visual depictions of the DAFH functions $\varphi_{i\Omega}$ for various domains in the molecule, alongside a consideration of the corresponding occupation numbers $n_{i\Omega}$, which provides insights into the chemical bonding, including direct links to familiar chemical concepts such as bonds, lone pairs and so on. The DAFH analysis detects any electron pairs that remain intact within a given domain and provides information about the broken or dangling valences that are created by the (formal) bond splitting that would be required to isolate that domain from the rest of the molecule. It straightforwardly elucidates the manner and the extent to which the electrons associated with a given domain (often an atom) are involved in interactions with those for other domains in the molecule.

As was mentioned in the Introduction, further integration of g_Ω over the same or a different domain generates localization and delocalization indices, respectively. Specifically, we may write:

$$k_{\Omega\Omega'} = \int\limits_{\substack{r_1 = r_1' \\ \Omega'}} g_\Omega(\boldsymbol{r}_1, \boldsymbol{r}_1')\,d\boldsymbol{r}_1 = \sum_{I,J} G_\Omega(I,J)S_{\Omega'}(I,J) = Trace(\mathbf{G}_\Omega\mathbf{S}_{\Omega'})$$

(5)

and then define 'diagonal' (*i.e.* one-domain) elements $SEDI(\Omega,\Omega) = k_{\Omega\Omega}$ and the corresponding off-diagonal (*i.e.* two-domain) quantities $SEDI(\Omega,\Omega') = k_{\Omega\Omega'} + k_{\Omega'\Omega}$. It follows from equations 3 and 5 that the values of $k_{\Omega\Omega}$ and $k_{\Omega\Omega'}$ (and thus SEDI) can straightforwardly be expressed [27] (see also [12,13]) as the simple summation of terms P_i that involve individual DAFH functions $\varphi_{i\Omega}$. These P_i are very straightforward to compute given the following expression:

$$P_i(\Omega,\Omega') = n_{i\Omega}\sum_{I,J} d_{i\Omega I}d_{i\Omega J}S_{\Omega'}(I,J)$$

(6)

We turn now to the FALDI-like approach, which involves the generation of the eigenfunctions and corresponding eigenvalues of $\mathbf{G}_\Omega\mathbf{S}_{\Omega'}$ rather than those of $\mathbf{G}_\Omega$. Whereas the matrices $\mathbf{G}_\Omega$ and $\mathbf{S}_{\Omega'}$ are symmetric, their product $\mathbf{G}_\Omega\mathbf{S}_{\Omega'}$ need not be (unless $\mathbf{G}_\Omega$ and $\mathbf{S}_{\Omega'}$ commute) and so $\mathbf{G}_\Omega\mathbf{S}_{\Omega'}$ can exhibit different sets of left- and right-hand eigenvectors, albeit with the same eigenvalues. Instead of solving directly the right-hand FALDI-like eigenvalue equation, namely

$$(G_\Omega S_{\Omega'}) x_{\Omega\Omega'} = \lambda_{\Omega\Omega'} x_{\Omega\Omega'}$$

(7)

or the corresponding left-hand FALDI-like eigenvalue problem

$$y_{\Omega\Omega'}^T (G_\Omega S_{\Omega'}) = \lambda_{\Omega\Omega'} y_{\Omega\Omega'}^T$$

(8)

we can in principle recast both of these equations in the more convenient symmetric form:

$$\left(S_{\Omega'}^{\frac{1}{2}} G_\Omega S_{\Omega'}^{\frac{1}{2}}\right) z_{\Omega\Omega'} = \lambda_{\Omega\Omega'} z_{\Omega\Omega'}$$

(9)

with $x_{\Omega\Omega'} = S_{\Omega'}^{-\frac{1}{2}} z_{\Omega\Omega'}$ and $y_{\Omega\Omega'} = S_{\Omega'}^{\frac{1}{2}} z_{\Omega\Omega'}$. It is of course straightforward to generate $S_{\Omega'}^{\frac{1}{2}}$ from the symmetric matrix $S_{\Omega'}$ and, provided that $S_{\Omega'}$ is also positive definite, we can also easily generate $S_{\Omega'}^{-\frac{1}{2}}$. A simple pragmatic alternative to the use of equations 7 to 9 is to find instead the eigenvectors and corresponding eigenvalues of the following symmetric problem:

$$\frac{1}{2}(G_\Omega S_{\Omega'} + S_{\Omega'} G_\Omega) v_{\Omega\Omega'} = \lambda_{\Omega\Omega'}^s v_{\Omega\Omega'}$$

(10)

We note that such a strategy does in fact mimic the approach adopted in the original FALDI studies [15-19] that were based on a one-electron approximation to G_Ω.

Regardless of which of equations 7 to 10 we use, the eigenvalues must sum to $k_{\Omega\Omega'}$ (see equation 5) so that we can easily identify the principal contributions to a given SEDI value. In common with what is done in DAFH analysis, we have chosen here to carry out a subsequent isopycnic transformation [20] of the corresponding eigenvectors and then to analyze the transformed functions with the largest eigenvalues. The full sets of eigenvalues will of course still sum to $k_{\Omega\Omega'}$ in each case and the sum of all diagonal (*i.e.* one-domain) and off-diagonal (*i.e.* two-domain) k values for a given system must still match the trace of the one-electron density matrix, *i.e.* the number of active electrons. It is important to note a fundamental difference between the DAFH and FALDI-like approaches when it comes to the individual contributions to these different k values. On the one hand, FALDI and FALDI-like approaches involve solving separate one-domain and two-domain eigenvalue problems, thereby generating two different sets of functions, with the former related only to diagonal k values and the latter only to off-diagonal k values. On the other hand, DAFH functions, which are obtained from one-domain eigenvalue problems, contribute (whether significantly or not) both to diagonal and off-diagonal k values.

It is useful to notice that whereas full DAFH analysis requires construction of the matrix representation G_Ω of the 'hole' g_Ω, as was described earlier, we can regenerate that matrix with minimal effort when we then go on to the FALDI-like analysis. This is because we can identify from equation 3 that

$$G_\Omega(I,J) = \sum_i n_{i\Omega} d_{i\Omega I} d_{i\Omega J}$$

(11)

which involves little more than the calculation of dot products. (Note that it is important in the summations in equations 3 and 11 to include all of the functions, labelled by i, whether or not they were actually included in the isopycnic transformation, which deals only with non-negative eigenvalues [20].)

In order to provide answers to various questions posed in the Introduction, we first examine the breaking of the single bond in H_2 so as to compare DAFH analysis with variants of FALDI-like approaches. We also examine the geometry dependence of the reliability of the usual one-electron approximation to the full treatment. We then do much the same for the breaking of the formal triple bond in N_2, not least to discover whether various observations for H_2 also apply for higher bond multiplicity. Finally, we use B_2H_6 near its equilibrium geometry as an example that features bonds that are not only heteronuclear but that also involves a bonding pattern which transcends the conventional two-center paradigm. It is also useful to note that whereas the isopycnic transformation actually does relatively little to the DAFH eigenfunctions and eigenvalues in the cases of H_2 and N_2, it does somewhat more in the case of B_2H_6; these observations also turn out to be true for the FALDI-like approaches we considered. It is important to stress that our emphasis in the present work is on the testing of (combinations of) methodologies rather than on looking for new insights into the electronic structure and bonding in the chosen intentionally familiar molecular systems.

It is also important to notice that whereas for the DAFH and diagonal FALDI-like approaches we solve a separate eigenvalue problem for each domain Ω in turn, the off-diagonal FALDI-like case does of course involve two such domains, Ω and Ω'. Although $k_{\Omega\Omega'}$ and $k_{\Omega'\Omega}$ must coincide, the FALDI-like partitioning of them leads to two different sets of functions. Depending on their forms, we can thus expect to be able to identify (by visual inspection) the FALDI-like functions which are mostly associated with one domain (Ω) or with the other one (Ω'). For homonuclear systems, such as H_2 and N_2, the functions in the two sets are trivially related to one another by symmetry. On the other hand, for (say) a B−H bond in a system such as B_2H_6, the two sets of functions will be different from one another so that, depending on the forms of the functions, we can say that they provide a view of the bonding from either the B or the H perspective.

As is well known, a variety of definitions of bond orders have proved to be especially useful in attempts to understand electronic structure and bonding, with variants of the Wiberg-Mayer (W-M) index being particularly widely used. For the special case of correlated singlet systems, Mayer introduced a so-

called 'improved' definition [30] of such a two-center W-M index which, when re-expressed in QTAIM-generalized form [31], can be written [32]:

$$\text{W-M}(\Omega, \Omega') = \sum_I \sum_J \left(\omega_I \omega_J + \left[\omega_I (2 - \omega_I) \omega_J (2 - \omega_J) \right]^{\frac{1}{2}} \right) S_\Omega(I,J) \, S_{\Omega'}(I,J)$$

(12)

It proves useful for the bond breaking in H_2 and N_2 to compare the geometry dependence of $\text{W-M}(\Omega, \Omega')$ and $\text{SEDI}(\Omega, \Omega')$

We used here full configuration interaction (FCI) descriptions of H_2 based on a standard cc-pVTZ basis. In practice, these FCI/cc-pVTZ wavefunctions for H_2 were generated for a range of nuclear separations (R) by means of '2 electrons in 28 orbitals' complete active space self-consistent field (CASSCF) calculations. We also used standard cc-pVTZ basis sets, always in spherical form, for the other systems we studied, with all of the various calculations carried out in D_{2h} symmetry. In the case of N_2 we employed full-valence CASSCF ('10 electrons in 8 orbitals') descriptions, again for a range of nuclear separations, and we also carried out full-valence CASSCF ('12 electrons in 14 orbitals') calculations for B_2H_6 near its equilibrium geometry. (The coordinates used for the symmetry-unique atoms are available in Table S1 in the electronic supplementary material.) All of the wavefunctions required for the present work were calculated using MOLPRO [33,34] and the subsequent DAFH, FALDI-like, SEDI and bond order analysis including isopycnic transformations used our own codes, with the QTAIM analysis [21] carried out with AIMAll [35]. Using the same isovalue throughout, pictorial depictions of DAFH and FALDI-like functions were produced using Virtual Reality Markup Language (VRML) files generated with Molden [36].

4 Results and discussion

We start with an examination of the bond breaking process in H_2. Then, taking account of what we find for H_2, we carry out similar analysis for the breaking of the formal triple bond in N_2 before moving on to consider the bonding situation in B_2H_6.

H_2

The geometry dependence of (off-diagonal) SEDI values and of the results of DAFH analysis for H_2 have been described in detail several times. In particular, wavefunctions at exactly the same level of theory as used in the present work were deployed by Cooper and Ponec [14] to show how combinations of DAFH and bond order analysis can be used to provide insights into the electron reorganization that accompanies the making and breaking of chemical bonds.

10

We report in Table 1 the values of $\text{SEDI}(\text{H}, \text{H}')$ as a function of R, calculated using the full methodology as well as with the usual one-electron approximation. (Given that $\text{SEDI}(\text{H}, \text{H}) + \frac{1}{2}\,\text{SEDI}(\text{H}, \text{H}') = 1$ in this case, the diagonal SEDI elements provide no additional information.) We observe that the sign of the errors introduced for this system by the one-electron approximation is consistent throughout and that the magnitudes remain rather small, increasing to no more than 1.1% for the largest of the R values that we have considered. Also reported in Table 1 are values of the QTAIM-generalized 'improved' W-M index, as defined in equation 12. We observe that the reduction in the value of $\text{SEDI}(\text{H}, \text{H}')$ with increasing R is similar to the corresponding behavior of the W-M index, although the two curves are not parallel. Even so, it is clear that $\text{SEDI}(\text{H}, \text{H}')$ behaves very much like a bond order.

Dominant DAFH functions associated with the domain of one of the H atoms in H_2 are shown in Figure 1 for three representative values of R. As in previous work, we use here the term 'dominant functions' to signify all of those with eigenvalues (or occupation numbers) of at least 0.1. Also displayed in Figure 1 for each function is the corresponding occupation number as well as the proportion of $k_{\text{HH}'} = \frac{1}{2}\,\text{SEDI}(\text{H}, \text{H}')$ that is contributed by the value of P_i (see equation 6). Quoting these proportions (expressed as percentages) rather than the actual numerical values of P_i proves to be somewhat more convenient for direct comparisons with the corresponding results when using instead the one-electron approximation. In each case, the occupation number is fairly close to unity and the proportion of $k_{\text{HH}'}$ is very high. As can be seen from Figure S1 in the electronic supplementary material, the analogous DAFH functions and numerical values generated using the one-electron approximation are quite similar to those presented here for the full calculation.

Near equilibrium geometry, the dominant DAFH function for each H atom domain has an occupation close to unity (0.992). These two functions have a high overlap (0.984), with each of them resembling a slightly asymmetric version of a $1\sigma_g$ molecular orbital. Clearly such a DAFH description corresponds rather closely to an almost doubly occupied $1\sigma_g$ orbital. This is of course consistent with the occupation number of the corresponding natural orbital, which is also close to two (1.964). Increasing the nuclear separation leads to further asymmetry in the dominant DAFH functions and to a reduction in the overlap between them, corresponding to a decrease in the extent of sharing, but it has relatively little effect on their occupation numbers (which gradually move slightly closer to unity).

Of course, from a purist point of view, there is something slightly unsettling about some of these results not least because, in the absence of same-spin interactions, there can be no Fermi hole [37]. Nonetheless the DAFH analysis does lead to functions that can easily be interpreted in terms of the

R-dependence of the bonding and to values of $SEDI(H, H')$ which, in general terms, display the sort of behavior anticipated for a bond index.

We now turn to the results of the FALDI-like approaches, for which we have considered the four variants introduced above:

    A. Direct use of $\boldsymbol{z}_{\Omega\Omega'}$ and $\lambda_{\Omega\Omega'}$ from the solution of equation 9.

    B. Use of $\boldsymbol{v}_{\Omega\Omega'}$ and $\lambda^s_{\Omega\Omega'}$ from the artificially symmetrized problem in equation 10.

    C. Use of the left-hand eigenvectors $\boldsymbol{x}_{\Omega\Omega'} = \mathbf{S}_{\Omega'}^{-\frac{1}{2}}\boldsymbol{z}_{\Omega\Omega'}$ following solution of equation 9.

    D. Use of the right-hand eigenvectors $\boldsymbol{y}_{\Omega\Omega'} = \mathbf{S}_{\Omega'}^{\frac{1}{2}}\boldsymbol{z}_{\Omega\Omega'}$ following solution of equation 9.

For the same nuclear separations as were considered in Figure 1, the resulting dominant FALDI-like functions that can be associated (by visual inspection) with the domain of one of the H atoms are shown in Figure 2 together with their eigenvalues and the relative contributions to the relevant k values. For each value of R, the first row corresponds to partitioning of the (diagonal, *i.e.* one-domain) k_{HH} value and the second one to the corresponding partitioning of the (off-diagonal, *i.e.* two-domain) $k_{HH'}$ value. The columns are labelled A-D according to the variant of the approach that was used. As can be seen from Figure S2 in the electronic supplementary material, the analogous results when using the one-electron approximation are rather similar to those presented here for the full calculation.

An immediate observation from Figure 2 is that scheme B, namely use of the artificially symmetrized problem (equation 10), can produce eigenvalues that exceed the relevant k values. They are of course balanced by contributions from functions with negative eigenvalues, but the fact that the dominant functions can contribute more than 100% seems to be an unwelcome distraction. As such, we do not consider any further the results for H_2 from scheme B. For somewhat different reasons, we also do not dwell on the results for H_2 from scheme D, namely use of the right-hand eigenvectors $\boldsymbol{y}_{\Omega\Omega'} = \mathbf{S}_{\Omega'}^{\frac{1}{2}}\boldsymbol{z}_{\Omega\Omega'}$ following solution of equation 9. This is because the forms of these functions turn out to be rather similar to those from the DAFH analysis and so it seems unlikely that the results of scheme D will provide much additional information. This leaves us with Schemes A and C, for which the two sets of results turn out to be rather similar. From a purely computational point of view, Scheme A (direct use of the functions from the solution of equation 9) is slightly preferable to Scheme C because it avoids the requirement to generate $\mathbf{S}_{\Omega'}^{-\frac{1}{2}}$ (as would be required for the construction of $\boldsymbol{x}_{\Omega\Omega'} = \mathbf{S}_{\Omega'}^{-\frac{1}{2}}\boldsymbol{z}_{\Omega\Omega'}$ in Scheme C).

Focusing on the results of Scheme A, we observe in each case that the dominant FALDI-like function for a given value of R accounts for a high proportion ($> 97\%$) of the relevant k value. Except for the largest of the three nuclear separations considered in Figure 2, the dominant functions from the partitioning of diagonal (*i.e.* one-domain) and off-diagonal (*i.e.* two-domain) k values are remarkably

similar to one another. Looking first at the dominant function for the diagonal case (top row for each value of R) we notice that it becomes increasingly s-like at larger R and that it is somewhat more localized for all three R values than was the case for the corresponding DAFH functions. Turning now to the dominant FALDI-like functions for the off-diagonal case, we notice that these are also somewhat more localized than are the corresponding DAFH functions, but that there is a deviation from pure s-like character for the largest value of R shown in Figure 2 – exactly the same behavior is observed for the Scheme C functions.

Having examined the breaking of the single bond in H_2 we can now move onto a comparison of our observations with those that we can make for the formal triple bond in N_2.

N_2

It is clear from the $SEDI(N, N')$ values for N_2 which are reported in Table 2 that the magnitudes of the errors introduced for this system by the one-electron approximation are somewhat larger than was the case for H_2, as might have been anticipated from the larger number of electrons. Furthermore the errors show much more dependence on R for breaking the formal triple bond in N_2 than they do for the single bond in H_2. An error of 18% near the equilibrium geometry of N_2 increases to 24% at intermediate R before changing sign at larger nuclear separations. Also reported in Table 2 are values of the 'improved' W-M index and we observe that the reduction in the value of $SEDI(N, N')$ in the region from 1.5Å to 2Å is somewhat more gradual than is the corresponding behavior of the W-M index. (Given for these calculations with 10 active electrons that $SEDI(N, N) + ½ SEDI(N, N') = 5$, the diagonal SEDI elements provide no additional information.)

Dominant DAFH functions associated with the domain of one of the N atoms are shown in Figure 3 for three representative values of R with the smallest of the three values (1.1Å) being close to R_e. Also displayed for each of these functions is the corresponding occupation number as well as the proportion of $k_{NN'} = ½ SEDI(N, N')$ that is contributed by the value of P_i (see equation 6). As can be seen from Figure S3 in the electronic supplementary material, the analogous DAFH functions and numerical values generated using the one-electron approximation are similar to those presented here for the full calculation.

It is clear from Figure 3 that we observe a consistent pattern for the dominant DAFH functions for N_2 at the different values of R. The first function, with an occupancy approaching two, resembles a nonbonding 'lone pair' σ function near equilibrium geometry and evolves into an s orbital at larger R. It accounts for ~50% of $k_{NN'} = ½ SEDI(N, N')$ near equilibrium, dropping towards 40% as the two atoms are moved apart. Next we observe a degenerate pair of functions of π symmetry, each with an occupation

13

number that is close to unity. Each of these functions accounts for 18% of ½ SEDI(N, N′) near the equilibrium geometry, but this proportion increases slightly as R is increased. Finally we observe another σ function, again with an occupancy that is close to unity. It evolves from a σ bonding function near equilibrium geometry into a $2p_z$ function at larger R. Although it contributes less than 16% of ½ SEDI(N, N′) near the equilibrium geometry, this proportion increases with R (albeit to a slightly larger fraction of a somewhat smaller total number).

For the same nuclear separations as were considered in Figure 3, the resulting dominant Scheme A FALDI-like functions that can be associated (by visual inspection) with the domain of one of the N atoms are shown in Figure 4 together with their eigenvalues as well as the relative contributions that these make to the relevant k values. The corresponding results when using instead Schemes B-D (see Figures S4-S6 in the electronic supplementary material) tell a familiar story: the combined contributions from the dominant Scheme B functions typically exceed 100%, the outcome of Scheme D is strongly reminiscent of the results of the DAFH analysis, and the results from Schemes A and C are rather similar to one another. The analogous functions and numerical values for Schemes A-D when using instead the one-electron approximation are observed in each case to be similar to those from the full calculations (see Figures S7-S10 in the electronic supplementary material).

Looking at the dominant Scheme A FALDI-like functions for the two-domain off-diagonal (NN′) case for R=1.1Å (near R_e), we observe in Figure 4 a σ function that accounts for nearly 40% of $k_{NN'}$ and then a pair of degenerate π functions, each of which accounts for nearly 30% of $k_{NN'}$. Moving on to R=1.5Å we find that the π functions become somewhat more localized on the relevant N atom domain and now contribute a slightly reduced proportion of $k_{NN'}$, with an increase to 45% for the σ function. It is clear for both of these values of R that the dominant Scheme A FALDI-like functions provide a more efficient representation of $k_{NN'}$ than was the case for the corresponding DAFH functions. This is because just three FALDI-like functions (one σ and two π) account for most of $k_{NN'}$ whereas we require instead four DAFH functions (two σ and two π). Moving to larger R (2.5Å) the value of $k_{NN'}$ = ½ SEDI(N, N′) drops below 0.1 (see Table 2) and so it is not surprising that none of the Scheme A FALDI-like functions reached our chosen threshold (eigenvalue > 0.1) to be displayed.

Moving on to the one-domain diagonal (NN) case we observe from Figure 4 that there are striking similarities to the outcome of the DAFH analysis (see Figure 3). Indeed, the dominant Scheme A FALDI-like functions account for almost the same proportion of k_{NN} = SEDI(N, N) as did the DAFH functions for $k_{NN'}$ = ½ SEDI(N, N′). Focusing instead on the differences, we observe in particular that the

degenerate pair of π functions is much more localized to a single N atom domain that are the corresponding DAFH functions.

As our final example we move on to B_2H_6 near its equilibrium geometry. Not only does this system feature bonds between different atoms, unlike the cases of H_2 and N_2, but it also presents a bonding pattern that goes beyond the usual two-electron two-center paradigm.

B_2H_6

Various off-diagonal SEDI(Ω, Ω') values for B_2H_6 are reported in Table 3. The corresponding diagonal elements are also listed (last three rows of Table 3) for a terminal hydrogen atom (H_t), a bridging hydrogen atom (H_b) and for a boron atom. We have used primes to distinguish between atoms of the same type, such that SEDI$(H_t, H_{t'})$ corresponds to the value for two different terminal H atoms that are attached to the same boron center. For the directly bonded atoms, the error from use of the one-electron approximation is somewhat smaller than was the case for N_2, varying only from -1.4% to $+2.1\%$. On the other hand, it is certainly true that there are large deviations for some of the other cases but it is important to remember that the corresponding SEDI(Ω, Ω') values are actually very small, with the consequence being that large percentage changes correspond to rather small absolute changes. This is especially true for the case of SEDI(B, B').

The dominant DAFH functions for various QTAIM domains in B_2H_6 are depicted in the first column of Figure 5, together with occupation numbers and the proportion of a relevant $k_{\Omega\Omega'} = \frac{1}{2}$ SEDI(Ω, Ω') value. The function in the top row (occupation 1.526), which is for the domain of one of the terminal hydrogen atoms, represents the main contribution from that atom to one of the $B-H_t$ bonds and it accounts for nearly 94% of $\frac{1}{2}$ SEDI(B, H_t). The function in the second row (occupation 0.346), which is instead for the domain of the corresponding boron atom, is the complementary contribution to this $B-H_t$ bond and it accounts for over 95% of $\frac{1}{2}$ SEDI(B, H_t). (Notice also that 1.526+0.346 is almost 1.9, consistent with conventional notions of a two-center two-electron $B-H_t$ bond.) The function in the third row (occupation 0.192) is for the domain of the same boron atom and represents the main contribution from this center to the bonding that involves one of the bridging hydrogen atoms, but it only accounts for ~85% of $\frac{1}{2}$ SEDI(B, H_b). Finally, the function in the bottom row (occupation 1.419) is for the domain of that bridging hydrogen and it does of course represent the main contribution from that atom to the anticipated three-center two-electron (3c-2e) $B-H_b-B'$ bonding. (Notice also that 2×0.192+1.419 slightly exceeds 1.8, consistent with notions of 3c-2e bonding.) This function only accounts for ~79% of each $\frac{1}{2}$ SEDI(B, H_b) value, being somewhat more suited to the diagonal term SEDI(H_b, H_b), for which it accounts for 97.7%.

15

The dominant Scheme A FALDI-like functions are depicted in the second and third columns of Figure 5. The corresponding results using Schemes B-D (see Figures S11-S13 in the electronic supplementary material) again show that the dominant Scheme B functions tend to overestimate k values, that the outcome of Scheme D is strongly reminiscent of the results of the DAFH analysis, and that it is the results from Schemes A and C which are rather similar to one another. Additionally, the corresponding functions and numerical values for Schemes A-D when using instead the usual one-electron approximation are again similar to those from the full calculations (see Figures S14-S17 in the electronic supplementary material).

Looking first at the dominant Scheme A FALDI-like functions for the off-diagonal (*i.e.* two-domain) SEDI values (middle column of Figure 5), the top two functions correspond to one of the $B-H_t$ linkages, but seen from the H_t and B perspectives, respectively. Each function accounts for a high proportion of $\frac{1}{2}\,SEDI(B, H_t)$. In a similar fashion, the final two functions in the middle column correspond to one of the $B-H_b$ linkages, as seen from the B and H_b perspectives, but both functions account for a slightly lower proportion of $\frac{1}{2}\,SEDI(B, H_b)$ than was the corresponding case for $B-H_t$. Nonetheless, in general terms, we observe that the Scheme A FALDI-like functions do provide a slightly more efficient expansion of SEDI values that do those from the corresponding DAFH analysis. The third column of Figure 5 shows depictions of the dominant Scheme A FALDI-like functions for the diagonal (*i.e.* one-domain) cases, specifically H_t and H_b, each of which accounts for a high proportion of the relevant $SEDI(\Omega, \Omega)$ element. The largest eigenvalue for the B domain was below our usual cutoff (0.1) and so this function has not been shown. (It is for much the same reason that we have not depicted here the FALDI-like functions for the two-domain BB′ and HH′ cases.) We notice that the 'diagonal' FALDI-like functions shown in the third column of Figure 5 are rather reminiscent of the DAFH functions associated with the same atomic domains.

5 Conclusions

We have presented here a systematic comparison of the performance of two complementary methodologies, namely DAFH analysis and FALDI-like analysis, both of which aim to provide useful insights into electronic structure and bonding by means of partitioning the densities and/or the density matrices provided by contemporary calculations. Whereas DAFH analysis provides information about the role and the extent of electron sharing in bonding situations, the complementary FALDI-like picture is in some senses somewhat richer. In particular, FALDI-like analysis provides detailed insights into the

partitioning of localization and delocalization indices (collectively called SEDI) into contributions associated with individual domains and with pairs of domains, respectively.

We are now in a strong position to provide some answers to the series of interrelated questions that were posed in the Introduction. We wondered just how similar/different are the functions generated by the DAFH and FALDI-like approaches for a particular molecule at a given level of theory, and how similar/different are the corresponding eigenvalues. A minor complication is that $G_\Omega S_{\Omega'}$ need not be symmetric, so that we are faced with more than one FALDI-like scheme. A simple pragmatic approach (which we called Scheme B) of using instead $\frac{1}{2}(G_\Omega S_{\Omega'} + S_{\Omega'} G_\Omega)$ turns out not be wholly satisfactory because the combined contributions from the dominant functions often exceed 100%. The left-hand eigenfunctions of $G_\Omega S_{\Omega'}$ (Scheme D) do turn out to be rather similar to those generated by DAFH analysis, but the eigenvalues are somewhat different, in one case being a direct measure of the contribution to the relevant k value and in the other being an occupation number. On the other hand, the right-hand eigenfunctions of $G_\Omega S_{\Omega'}$ (Scheme C) are somewhat different so that they could, in principle, provide additional, complementary information that is not already available from the DAFH analysis. Our computationally preferred approach (Scheme A), which is based on the convenient symmetric form $S_{\Omega'}^{\frac{1}{2}} G_\Omega S_{\Omega'}^{\frac{1}{2}}$, produces results which are rather similar to those from Scheme C. The consequences of our findings as to which of the different variants of the FALDI-like approach are the most useful can of course now be carried back to implementations of the original FALDI scheme [15-19]. In the remainder of this discussion, we consider only FALDI-like Scheme A.

One aim of the FALDI-like approach is to provide a compact description corresponding to expansions of the SEDI values. As such, an obvious question is whether such expansions are more compact (or more 'efficient') than are those provided by DAFH analysis via the values of $P_i(\Omega, \Omega')$ calculated using equation 6. As might have been anticipated, we found for H atom domains in H_2 at each value of R that there is a single dominant DAFH function and that there is a single dominant FALDI-like function. Each of these accounts for most of the total $k_{HH'} = \frac{1}{2} SEDI(H, H')$ value but the proportions are slightly higher with the FALDI-like approach, especially for larger nuclear separations. In this sense, the preferred FALDI-like approach (Scheme A) could be said to provide a slightly more efficient expansion of two-domain SEDI values than does DAFH analysis.

The errors in $SEDI(\Omega, \Omega')$ values from use of the usual one-electron approximation turned out to be rather small (up to 1.1%) for breaking the formal single bond in H_2 and they all have the same sign. On the other hand, the situation turned out to be somewhat different for breaking the formal triple bond in N_2. Not only did an error of 18% near the equilibrium geometry increase to 24% at intermediate R, but

it then changed sign at larger nuclear separations. The corresponding errors at a fixed geometry of B_2H_6 were somewhat smaller for the directly bonded atoms, varying only from -1.4% to $+2.1\%$. Nonetheless, it turns out that the forms of the dominant DAFH and FALDI-like functions from a given Scheme show rather little sensitivity to use of the one-electron approximation. Furthermore, the differences in the *relative* importance of the different functions in the expansions of the non-trivial SEDI values (when expressed as percentages) were always small, regardless of the formal bond multiplicity or of variations in the nuclear separations.

Having now established which of the four FALDI-like variants that we have considered provides information that complements DAFH and bond order analysis, we are now in a strong position to deploy such a combination of techniques for studies of systems with unknown and/or controversial bonding patterns. Based on the various observation in the present work, our preference will be for the full treatments, whenever they are possible, but we do now have clear indications of the extents to which we can rely instead on the somewhat more convenient one-electron approximation.

References

1. Coulson CA (1960) Present State of Molecular Structure Calculations. Rev Mod Phys 32 (2):170-177. doi:10.1103/RevModPhys.32.170

2. Hamming RW (1962) Numerical Methods for Scientists and Engineers. McGraw-Hill, New York

3. Neese F, Atanasov M, Bistoni G, Maganas D, Ye S (2019) Chemistry and Quantum Mechanics in 2019: Give Us Insight and Numbers. J Am Chem Soc 141 (7):2814-2824. doi:10.1021/jacs.8b13313

4. Mitoraj MP, Michalak A, Ziegler T (2009) A Combined Charge and Energy Decomposition Scheme for Bond Analysis. J Chem Theory Comput 5 (4):962-975. doi:10.1021/ct800503d

5. Zhao L, von Hopffgarten M, Andrada DM, Frenking G (2018) Energy decomposition analysis. WIREs Comput Mol Sci 8 (3):e1345. doi:10.1002/wcms.1345

6. Ponec R (1997) Electron pairing and chemical bonds. Chemical structure, valences and structural similarities from the analysis of the Fermi holes. J Math Chem 21 (3):323-333. doi:10.1023/a:1019186806180

7. Ponec R, Cooper DL (2007) Anatomy of Bond Formation. Domain-Averaged Fermi Holes as a Tool for the Study of the Nature of the Chemical Bonding in Li_2, Li_4, and F_2. J Phys Chem A 111 (44):11294-11301. doi:10.1021/jp070817f

8. Ponec R, Cooper DL (2007) Anatomy of bond formation. Bond length dependence of the extent of electron sharing in chemical bonds from the analysis of domain-averaged Fermi holes. Faraday Discuss 135 (0):31-42. doi:10.1039/B605313K

9. Ponec R, Cooper DL, Savin A (2008) Analytic Models of Domain-Averaged Fermi Holes: A New Tool for the Study of the Nature of Chemical Bonds. Chem Eur J 14 (11):3338-3345. doi:10.1002/chem.200701727

10. Bultinck P, Cooper DL, Ponec R (2010) Influence of Atoms-in-Molecules Methods on Shared-Electron Distribution Indices and Domain-Averaged Fermi Holes. J Phys Chem A 114 (33):8754-8763. doi:10.1021/jp101707w

11. Tiana D, Francisco E, Blanco MA, Macchi P, Sironi A, Martín Pendás Á (2011) Restoring orbital thinking from real space descriptions: bonding in classical and non-classical transition metal carbonyls. Phys Chem Chem Phys 13 (11):5068-5077. doi:10.1039/C0CP01969K

12. Baranov AI, Ponec R, Kohout M (2012) Domain-averaged Fermi-hole analysis for solids. J Chem Phys 137 (21). doi:10.1063/1.4768920

13. Francisco E, Martín Pendás A, Costales A (2014) On the interpretation of domain averaged Fermi hole analyses of correlated wavefunctions. Phys Chem Chem Phys 16 (10):4586-4597. doi:10.1039/C3CP54513J

14. Cooper DL, Ponec R (2018) Insights into molecular electronic structure from domain-averaged Fermi hole (DAFH) and bond order analysis using correlated density matrices. In: Carbó-Dorca R, Chakraborty T (eds) Quantum Chemistry at the Dawn of the 21st Century. Apple Academic Press, New Jersey, pp 405-443

15. de Lange JH, Cukrowski I (2017) Toward Deformation Densities for Intramolecular Interactions without Radical Reference States Using the Fragment, Atom, Localized, Delocalized, and Interatomic (FALDI) Charge Density Decomposition Scheme. J Comput Chem 38 (13):981-997. doi:10.1002/jcc.24772

16. Cukrowski I, van Niekerk DME, de Lange JH (2017) Exploring fundamental differences between red- and blue-shifted intramolecular hydrogen bonds using FAMSEC, FALDI, IQA and QTAIM. Struct Chem 28 (5):1429-1444. doi:10.1007/s11224-017-0956-5

17. de Lange JH, van Niekerk DME, Cukrowski I (2018) FALDI-based decomposition of an atomic interaction line leads to 3D representation of the multicenter nature of interactions. J Comput Chem 39 (16):973-985. doi:10.1002/jcc.25175

18. de Lange JH, Cukrowski I (2018) Exact and exclusive electron localization indices within QTAIM atomic basins. J Comput Chem 39 (20):1517-1530. doi:10.1002/jcc.25223

19. de Lange JH, van Niekerk DME, Cukrowski I (2018) FALDI-based criterion for and the origin of an electron density bridge with an associated (3,-1) critical point on Bader's molecular graph. J Comput Chem 39 (27):2283-2299. doi:10.1002/jcc.25548

20. Cioslowski J (1990) Isopycnic orbital transformation and localization of natural orbitals. Int J Quantum Chem S24:15-28

21. Bader RFW (1990) Atoms in Molecules. A Quantum Theory. Oxford University Press, Oxford

22. Cooper DL, Ponec R (2008) A one-electron approximation to domain-averaged Fermi hole analysis. Phys Chem Chem Phys 10 (9):1319-1329. doi:10.1039/B715904H

23. Fradera X, Austen MA, Bader RFW (1999) The Lewis Model and Beyond. J Phys Chem A 103 (2):304-314. doi:10.1021/jp983362q

24. Outeiral C, Vincent MA, Martín Pendás Á, Popelier PLA (2018) Revitalizing the concept of bond order through delocalization measures in real space. Chem Sci 9 (25):5517-5529. doi:10.1039/C8SC01338A

25. Matito E, Sola M, Salvador P, Duran M (2007) Electron sharing indexes at the correlated level. Application to aromaticity calculations. Faraday Discuss 135:325-345. doi:10.1039/b605086g

26. Ponec R, Cooper DL (2005) Anatomy of bond formation. Bond length dependence of the extent of electron sharing in chemical bonds. THEOCHEM 727 (1):133-138. doi:10.1016/j.theochem.2005.02.032

27. Cooper DL, Ponec R, Kohout M (2015) Are orbital-resolved shared-electron distribution indices and Cioslowski covalent bond orders useful for molecules? Mol Phys 113 (13-14):1682-1689. doi:10.1080/00268976.2015.1004377

28. Müller AMK (1984) Explicit approximate relation between reduced two- and one-particle density matrices. Phys Lett A 105 (9):446-452. doi:10.1016/0375-9601(84)91034-X

29. Fulton RL (1993) Sharing of electrons in molecules. J Phys Chem 97 (29):7516-7529. doi:10.1021/j100131a021

30. Mayer I (2012) Improved definition of bond orders for correlated wave functions. Chem Phys Lett 544:83-86. doi:10.1016/j.cplett.2012.07.003

31. Ángyán JG, Loos M, Mayer I (1994) Covalent bond orders and atomic valence indices in the topological theory of atoms in molecules. J Phys Chem 98 (20):5244-5248. doi:10.1021/j100071a013

32. Cooper DL, Ponec R, Kohout M (2016) New insights from domain-averaged Fermi holes and bond order analysis into the bonding conundrum in C_2. Mol Phys 114 (7-8):1270-1284. doi:10.1080/00268976.2015.1112925

33. Werner H-J, Knowles PJ, Knizia G, Manby FR, Schütz M, Celani P, Györffy W, Kats D, Korona T, Lindh R, Mitrushenkov A, Rauhut G, Shamasundar KR, Adler TB, Amos RD, Bennie SJ, Bernhardsson A, Berning A, Cooper DL, Deegan MJO, Dobbyn AJ, Eckert F, Goll E, Hampel C, Hesselmann A, Hetzer G, Hrenar T, Jansen G, Köppl C, Lee SR, Liu Y, Lloyd AW, Ma Q, Mata RA, May AJ, McNicholas SJ, Meyer W, Miller III TF, Mura ME, Nicklass A, O'Neill DP, Palmieri P, Peng D, Pflüger K, Pitzer R, Reiher M, Shiozaki T, Stoll H, Stone AJ, Tarroni R, Thorsteinsson T, Wang M, Welborn M MOLPRO, version 2019.2, a package of ab initio programs. Cardiff, U. K., see www.molpro.net

34. Werner H-J, Knowles PJ, Knizia G, Manby FR, Schütz M (2012) Molpro: a general-purpose quantum chemistry program package. WIREs Comput Mol Sci 2 (2):242-253. doi:10.1002/wcms.82

35. Keith TA AIMAll (Version 19.10.12). TK Gristmill Software, Overland Park KS, USA, see aim.tkgristmill.com

36. Schaftenaar G, Noordik JH (2000) Molden: a pre- and post-processing program for molecular and electronic structures. Journal of Computer-Aided Molecular Design 14 (2):123-134. doi:10.1023/a:1008193805436

37. Acke G, Bultinck P (2018) The influence of correlation on (de)localization indices from a valence bond perspective. J Mol Model 24 (10):275. doi:10.1007/s00894-018-3808-3

Figure 1. Dominant DAFH functions associated with the domain of one of the H atoms in H_2 at three representative nuclear separations. Also shown for each function is the corresponding occupation number as well as the proportion of $k_{HH'} = \frac{1}{2}\,\text{SEDI}(H, H')$ which can be assigned to a term P_i (see equation 6) that involves this function.
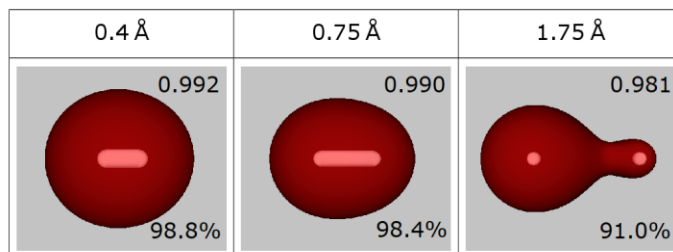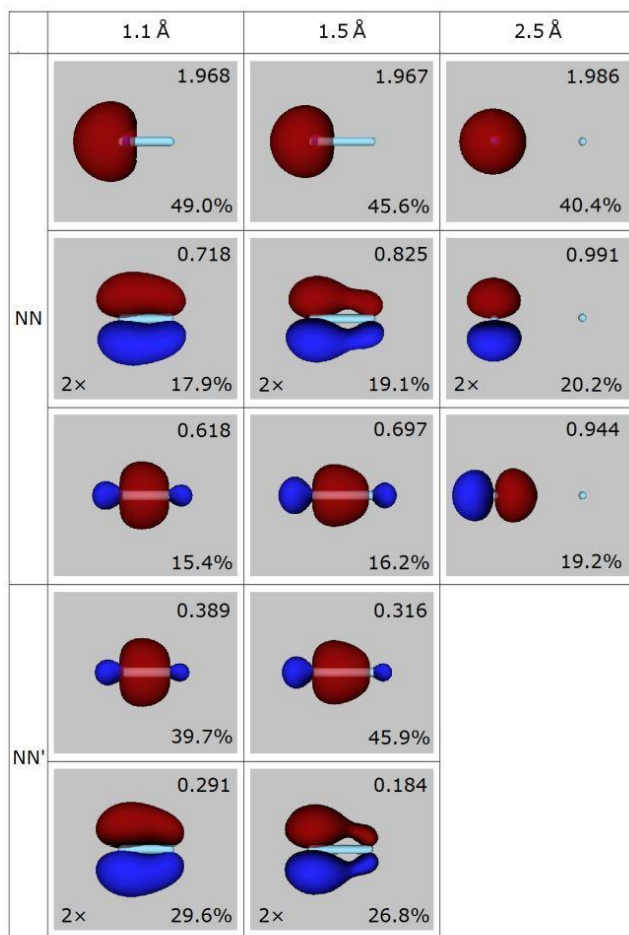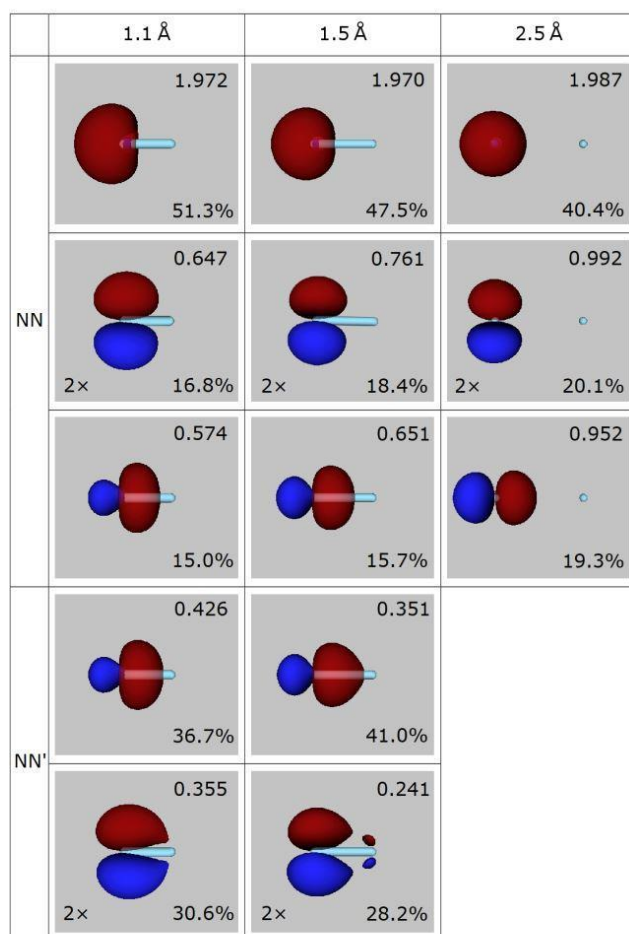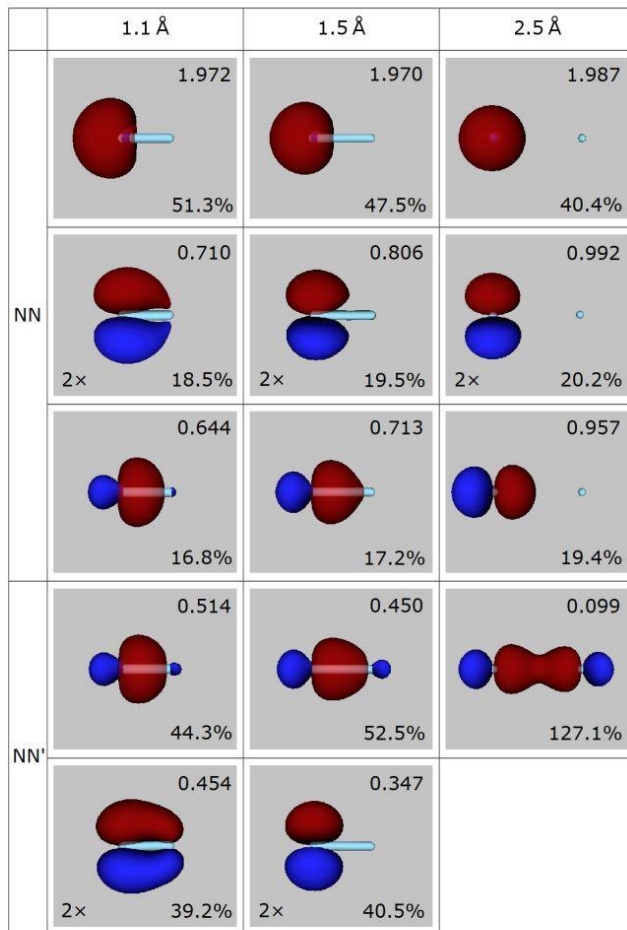
Figure 2. Dominant FALDI-like functions that can be associated (by visual inspection) with the domain of one of the H atoms in H_2 at three representative nuclear separations, together with their eigenvalues and relative contributions to the relevant k values. For each of these values of R, the first row corresponds to partitioning of k_{HH} and the second one to partitioning of $k_{HH'}$. Columns are labelled A-D according to the variant of the approach, as described in the text.
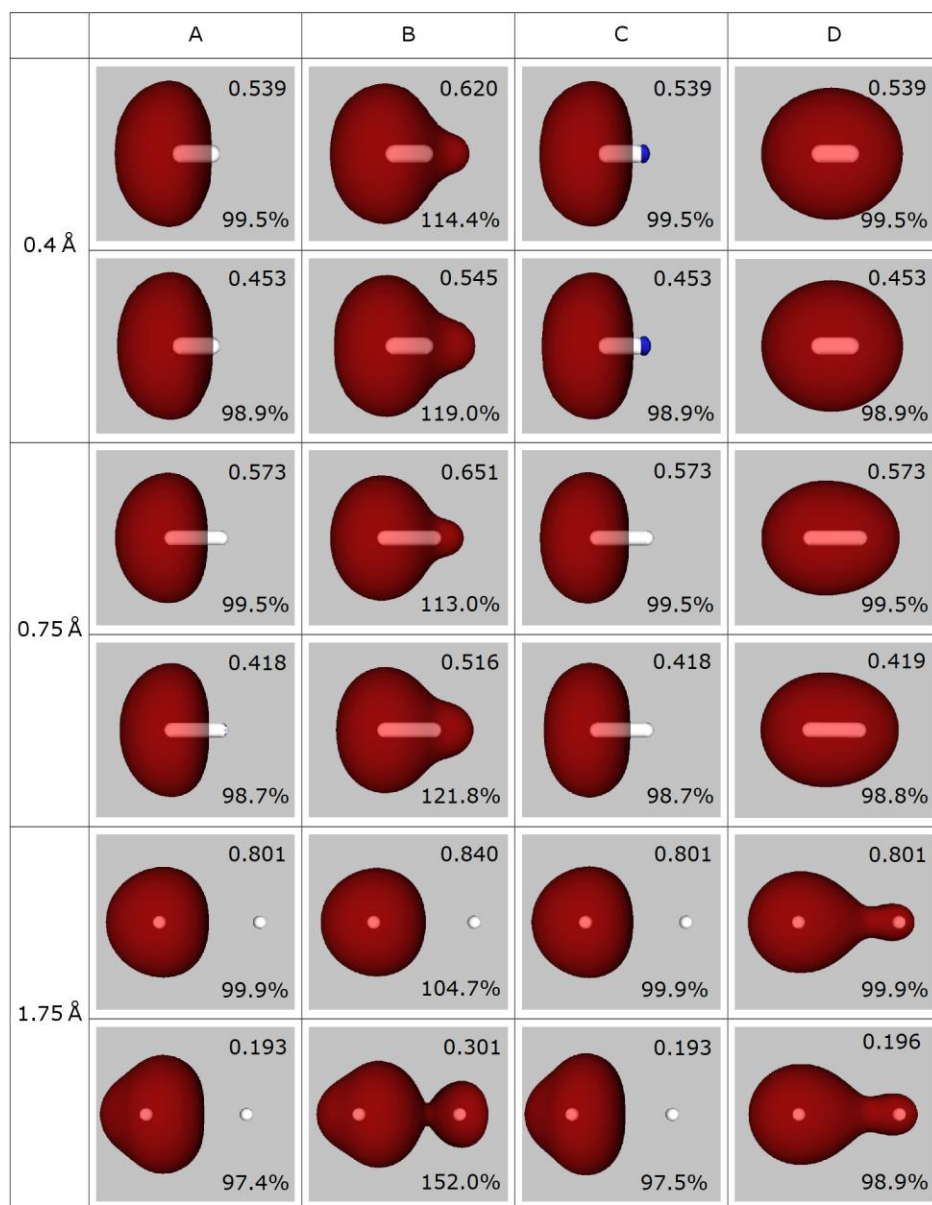
Figure 3. Dominant DAFH functions associated with the domain of one of the N atoms in N_2 at three representative nuclear separations. Also shown for each function is the corresponding occupation number as well as the proportion of $k_{NN'} = \frac{1}{2} \, SEDI(N, N')$ which can be assigned to a term P_i (see equation 6) that involves this function.
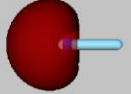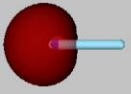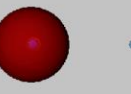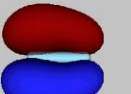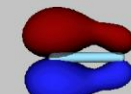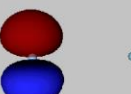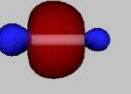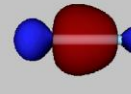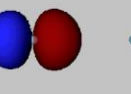
Figure 4. Dominant Scheme A FALDI-like functions that can be associated (by visual inspection) with the domain of one of the N atoms in N_2 at three representative nuclear separations, together with their eigenvalues and relative contributions to the relevant k values.
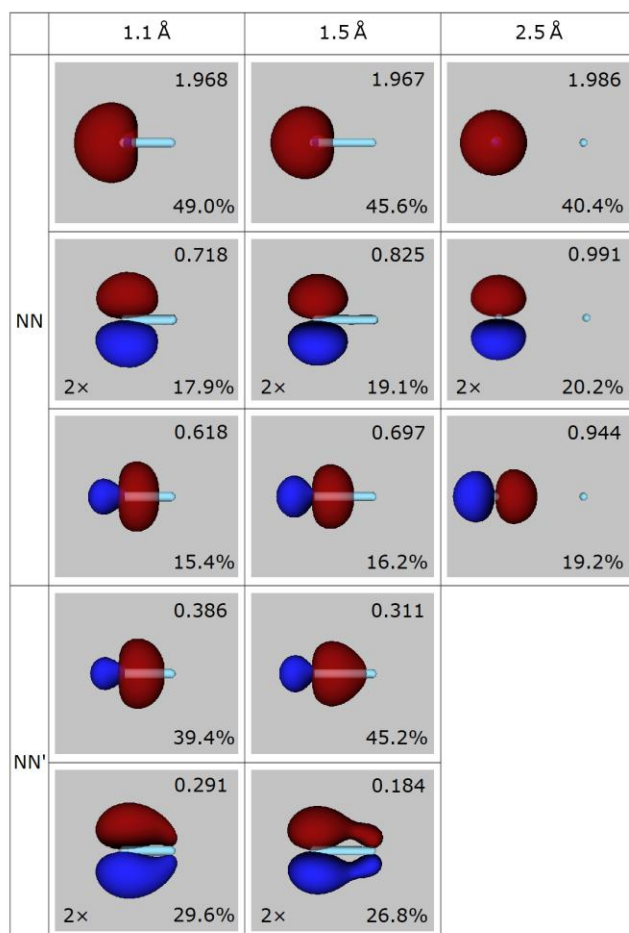
Figure 5. Dominant DAFH functions (first column) and Scheme A FALDI-like functions (second and third columns) for B_2H_6, together with their eigenvalues and relative contributions to relevant k values. The specific domains used for each of these functions are identified in the main text.
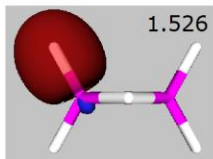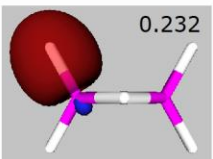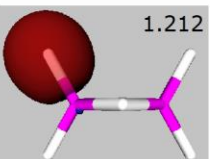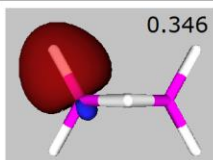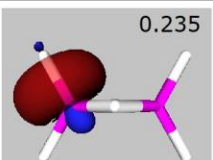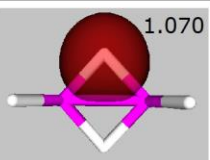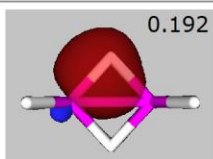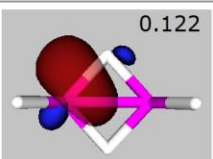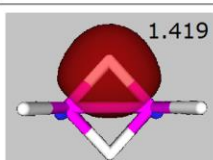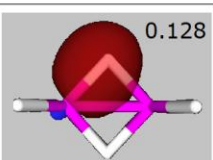
Table 1. Geometry dependence of off-diagonal (*i.e.* two-domain) SEDI values for H_2 and of the W-M bond order defined in equation 12.

R/Å	SEDI(H, H$'$)			W-M
	full	one-electron	error	
0.40	0.916	0.912	-0.4%	0.984
0.50	0.900	0.896	-0.5%	0.980
0.60	0.882	0.877	-0.5%	0.974
0.75	0.848	0.843	-0.6%	0.961
1.00	0.771	0.765	-0.8%	0.924
1.25	0.667	0.661	-0.9%	0.855
1.50	0.538	0.532	-1.0%	0.740
1.60	0.481	0.476	-1.1%	0.679
1.70	0.424	0.419	-1.1%	0.612
1.75	0.396	0.391	-1.1%	0.577
1.80	0.368	0.364	-1.1%	0.541

Table 2. Geometry dependence of off-diagonal (*i.e.* two-domain) SEDI values for N_2 and of the W-M bond order defined in equation 12.

R/Å	SEDI(N, N')			W-M
	full	one-electron	error	
0.95	2.178	2.492	14.4%	2.917
1.00	2.107	2.436	15.6%	2.887
1.10	1.963	2.318	18.1%	2.819
1.20	1.817	2.190	20.5%	2.738
1.30	1.671	2.050	22.7%	2.637
1.50	1.376	1.713	24.5%	2.341
1.70	1.064	1.264	18.8%	1.830
1.90	0.731	0.761	4.1%	1.133
2.10	0.455	0.420	-8.3%	0.610
2.50	0.176	0.156	-12.9%	0.201

Table 3. Off-diagonal (*i.e.* two-domain) SEDI values for B_2H_6, with the corresponding diagonal (*i.e.* one-domain) values shown in the last three rows.

domains	SEDI(Ω, Ω')		
	full	one-electron	error
B, H_t	0.484	0.495	2.1%
B, H_b	0.291	0.287	-1.4%
H_b, $H_{b'}$	0.179	0.187	4.9%
H_t, $H_{t'}$	0.116	0.107	-8.9%
H_b, H_t	0.099	0.096	-3.5%
B, B′	0.027	0.048	78.6%
H_t	1.222	1.230	0.7%
H_b	1.095	1.101	0.6%
B	0.234	0.214	-9.3%

Electronic supplementary material

Comparison of DAFH and FALDI-like approaches

David L. Cooper[1] • Jurgens de Lange[2] • Robert Ponec[3]

✉ David L. Cooper

dlc@liverpool.ac.uk

✉ Jurgens de Lange

jurgens.delange@up.ac.za

✉ Robert Ponec

ponec@icpf.cas.cz

1   Department of Chemistry, University of Liverpool, Liverpool L69 7ZD, UK

2   Theoretical Chemistry, Department of Chemistry, Faculty of Natural and Agricultural Sciences, University of Pretoria, Gauteng, South Africa

3   Institute of Chemical Process Fundamentals, Czech Academy of Sciences Prague 6, Suchdol 2, 165 02 Czech Republic

Section S1.   Geometry for B_2H_6

Table S1   Cartesian coordinates (in Å) used for symmetry-unique atoms in B_2H_6 (D_{2h}), with the inversion center taken as the origin. H_b is a bridging H atom and H_t is a terminal one.

Atom	x	y	z
B	0.888375	0	0
H_b	0	0	0.973751
H_t	1.463157	1.035737	0

Section S2.   Additional results for H_2

Figure S1.   Dominant DAFH functions associated with the domain of one of the H atoms in H_2 at three representative nuclear separations, generated using the one-electron approximation. Also shown for each function is the corresponding occupation number as well as the proportion of $k_{HH'} = \frac{1}{2} \text{SEDI}(H, H')$ which can be assigned to a term P_i (see equation 6) that involves this function.
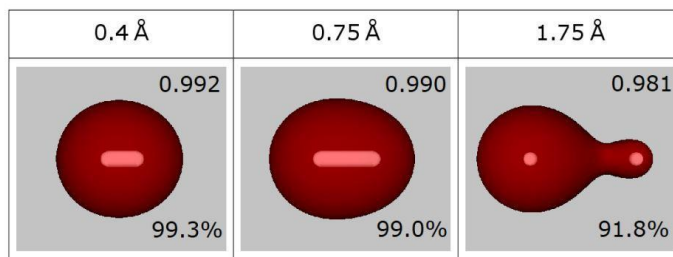
Figure S2. Dominant FALDI-like functions associated with the domain of one of the H atoms in H_2 at three representative nuclear separations, together with their eigenvalues and relative contributions to the relevant k values, calculated using the one-electron approximation. For each of these values of R, the first row corresponds to partitioning of k_{HH} and the second one to partitioning of $k_{HH'}$. Columns are labelled A-D according to the variant of the approach, as described in the text.
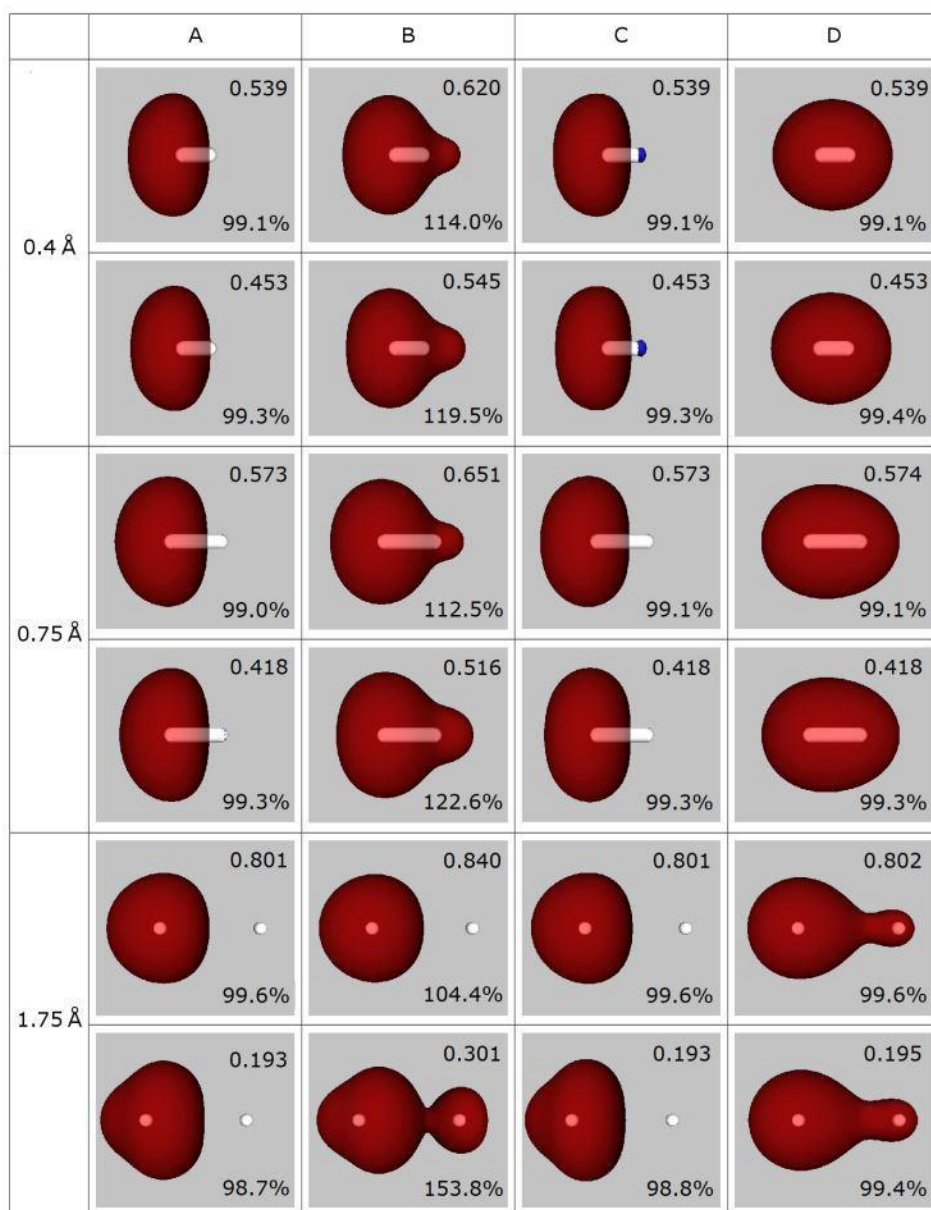
Section S3.   Additional results for N_2

Figure S3.   Dominant DAFH functions associated with the domain of one of the N atoms in N_2 at three representative nuclear separations, generated using the one-electron approximation. Also shown for each function is the corresponding occupation number as well as the proportion of $k_{NN'} = \frac{1}{2}\,SEDI(N, N')$ which can be assigned to a term P_i (see equation 6) that involves this function.
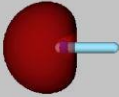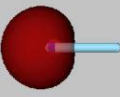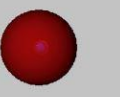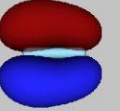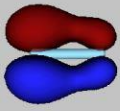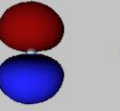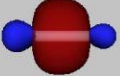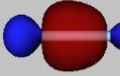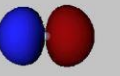
Figure S4.   Dominant Scheme B FALDI-like functions that can be associated (by visual inspection) with the domain of one of the N atoms in N_2 at three representative nuclear separations, together with their eigenvalues and relative contributions to the relevant k values, generated using the full calculation.
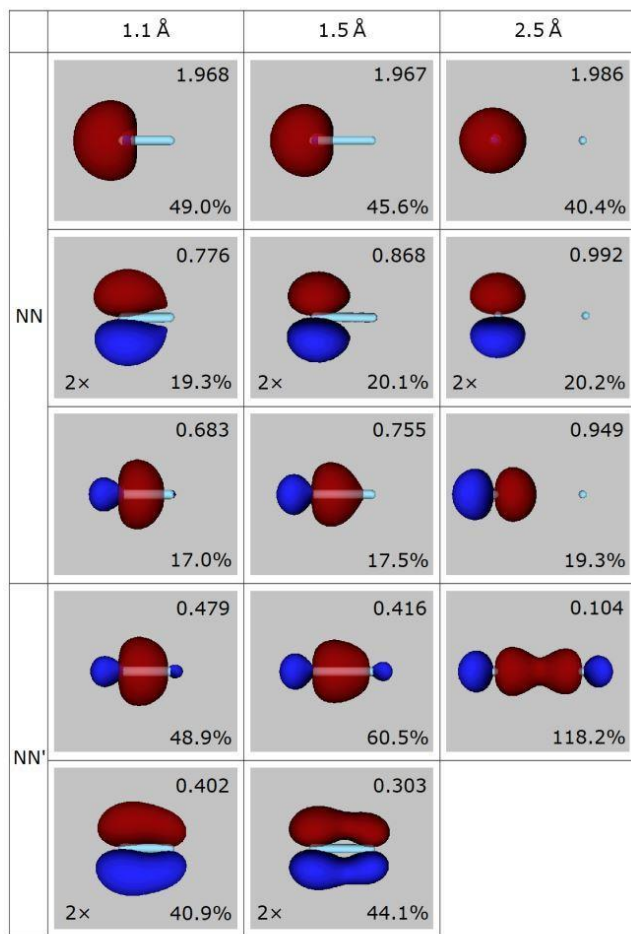
Figure S5.   Dominant Scheme C FALDI-like functions that can be associated (by visual inspection) with the domain of one of the N atoms in N_2 at three representative nuclear separations, together with their eigenvalues and relative contributions to the relevant k values, generated using the full calculation.
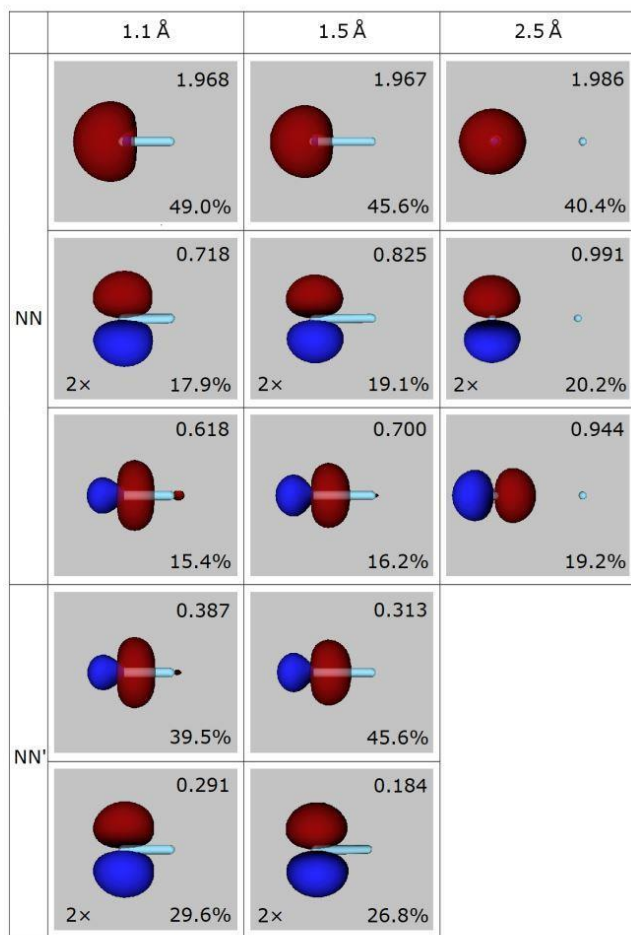
Figure S6. Dominant Scheme D FALDI-like functions that can be associated (by visual inspection) with the domain of one of the N atoms in N_2 at three representative nuclear separations, together with their eigenvalues and relative contributions to the relevant k values, generated using the full calculation.

Figure S7.   Dominant Scheme A FALDI-like functions that can be associated (by visual inspection) with the domain of one of the N atoms in N_2 at three representative nuclear separations, together with their eigenvalues and relative contributions to the relevant k values, calculated using the one-electron approximation.

Figure S8. Dominant Scheme B FALDI-like functions that can be associated (by visual inspection) with the domain of one of the N atoms in N_2 at three representative nuclear separations, together with their eigenvalues and relative contributions to the relevant k values, calculated using the one-electron approximation.

Figure S9.   Dominant Scheme C FALDI-like functions that can be associated (by visual inspection) with the domain of one of the N atoms in N_2 at three representative nuclear separations, together with their eigenvalues and relative contributions to the relevant k values, calculated using the one-electron approximation.
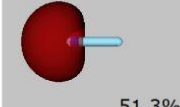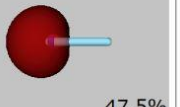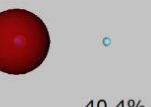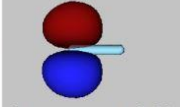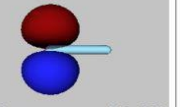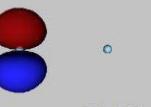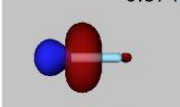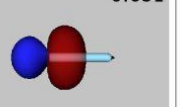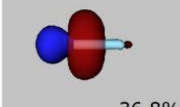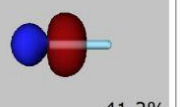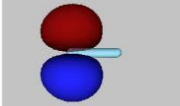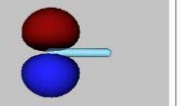
Figure S10. Dominant Scheme D FALDI-like functions that can be associated (by visual inspection) with the domain of one of the N atoms in N_2 at three representative nuclear separations, together with their eigenvalues and relative contributions to the relevant k values, calculated using the one-electron approximation.
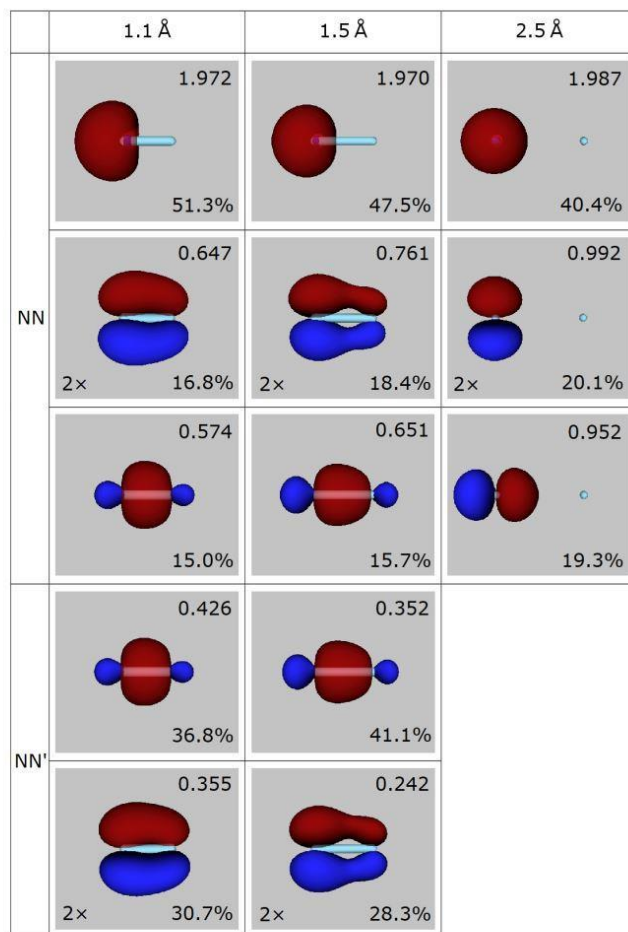
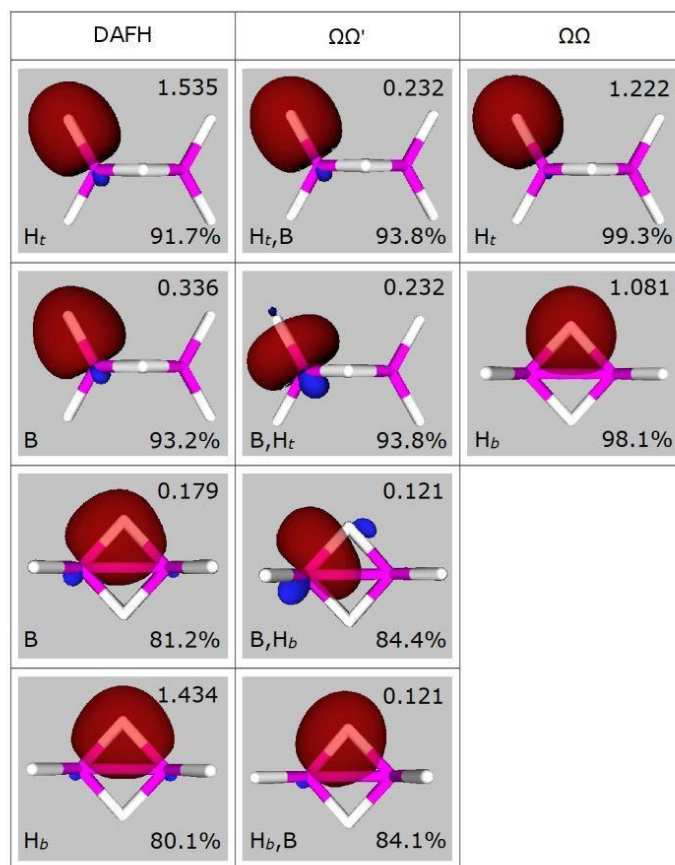# Section S4.   Additional results for B_2H_6

Figure S11.   Dominant DAFH functions (first column) and Scheme B FALDI-like functions (second and third columns) for B_2H_6, together with their eigenvalues and relative contributions to relevant k values, generated using the full calculation. The specific domains used for each of these functions are the same as those in Figure 5 and are identified in the main text, expect that the additional function depicted in the third column is associated with one of the B domains.
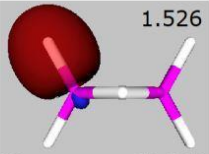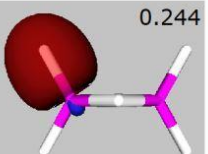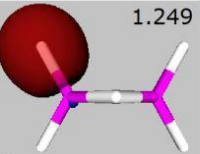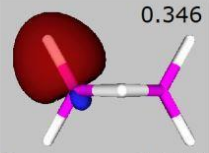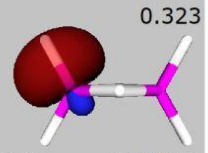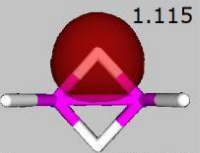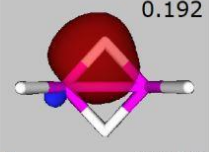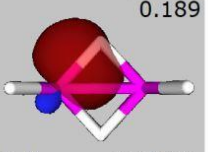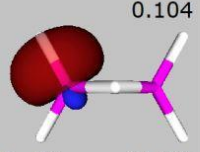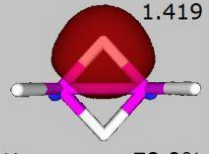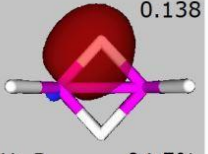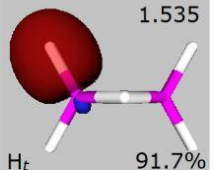
Figure S12. Dominant DAFH functions (first column) and Scheme C FALDI-like functions (second and third columns) for B_2H_6, together with their eigenvalues and relative contributions to relevant k values, generated using the full calculation. The specific domains used for each of these functions are the same as those in Figure 5 and are identified in the main text.
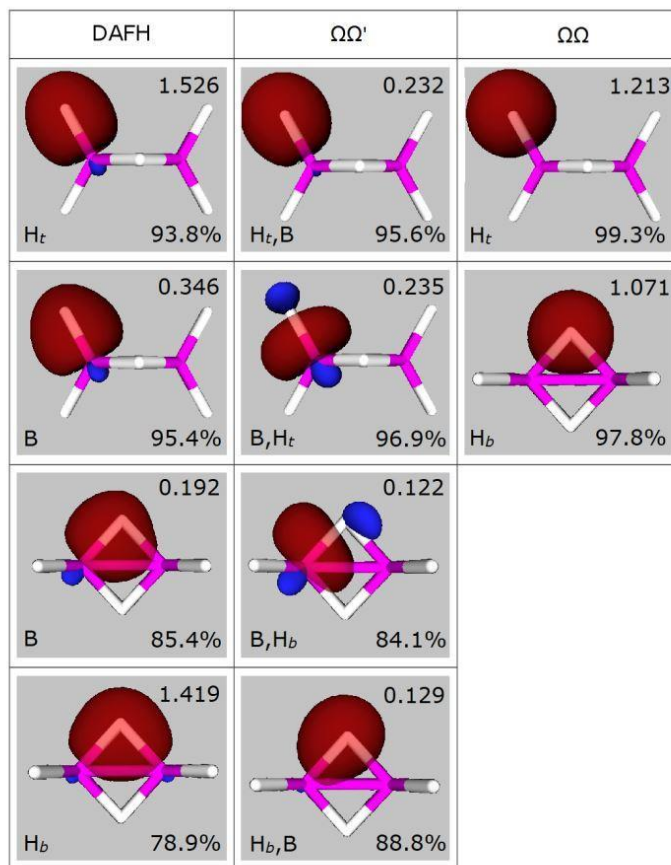
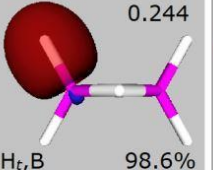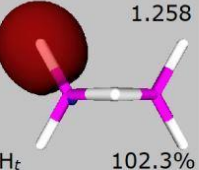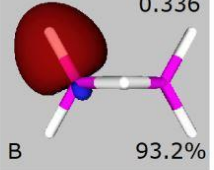Figure S13. Dominant DAFH functions (first column) and Scheme D FALDI-like functions (second and third columns) for B_2H_6, together with their eigenvalues and relative contributions to relevant k values, generated using the full calculation. The specific domains used for each of these functions are the same as those in Figure 5 and are identified in the main text.
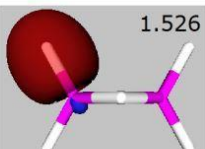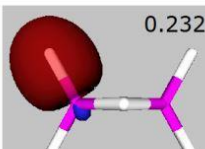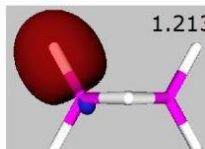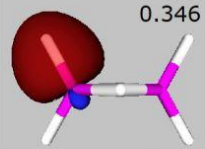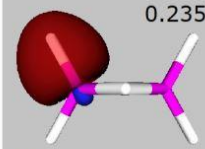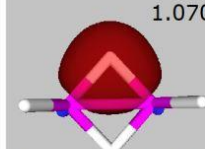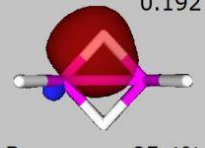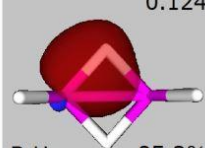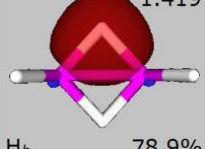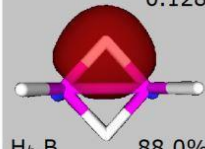
Figure S14.   Dominant DAFH functions (first column) and Scheme A FALDI-like functions (second and third columns) for B_2H_6, together with their eigenvalues and relative contributions to relevant k values, calculated using the one-electron approximation. The specific domains used for each of these functions are the same as those in Figure 5 and are identified in the main text.

Figure S15. Dominant DAFH functions (first column) and Scheme B FALDI-like functions (second and third columns) for B_2H_6, together with their eigenvalues and relative contributions to relevant k values, calculated using the one-electron approximation. The specific domains used for each of these functions are the same as those in Figure 5 and are identified in the main text.
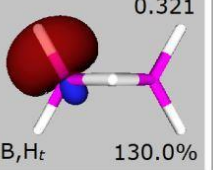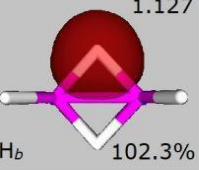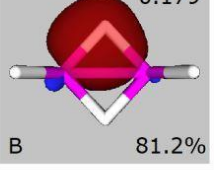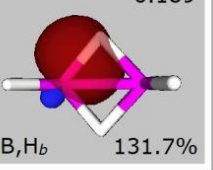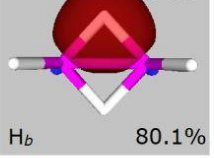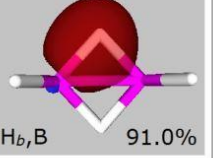
Figure S16.   Dominant DAFH functions (first column) and Scheme C FALDI-like functions (second and third columns) for B_2H_6, together with their eigenvalues and relative contributions to relevant k values, calculated using the one-electron approximation. The specific domains used for each of these functions are the same as those in Figure 5 and are identified in the main text.
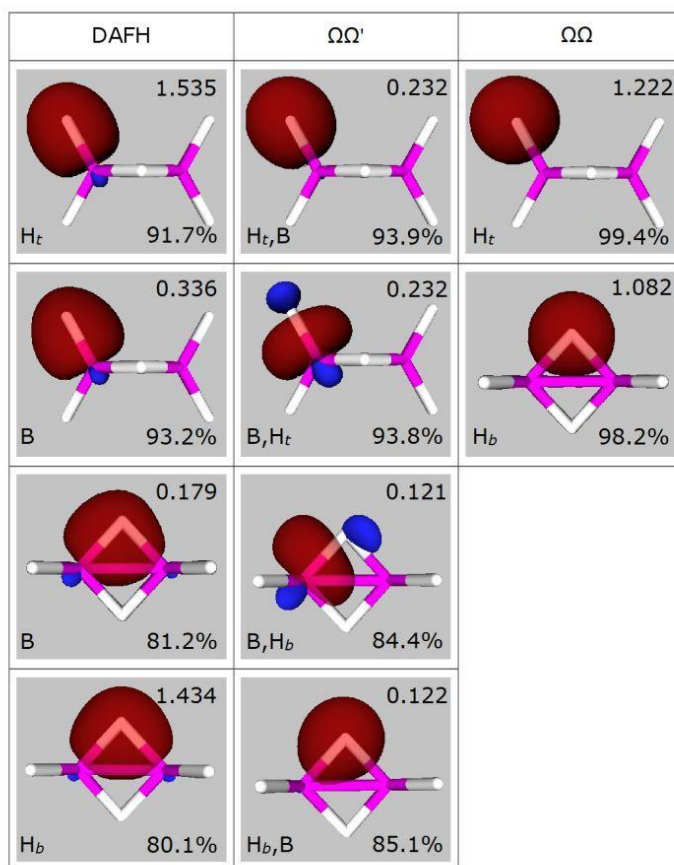
Figure S17. Dominant DAFH functions (first column) and Scheme D FALDI-like functions (second and third columns) for B_2H_6, together with their eigenvalues and relative contributions to relevant k values, calculated using the one-electron approximation. The specific domains used for each of these functions are the same as those in Figure 5 and are identified in the main text.